Kovove Mater. 50 2012 357–364
DOI: 10.4149/km_2012_5_357

Mechanical behavior of AISI 1045 steels subjected to powder-pack boriding

G. Rodríguez-Castro[1], I. Campos-Silva[1]*, J. Martínez-Trinidad[1], U. Figueroa-López[2], I. Arzate-Vázquez[3], E. Hernández-Sánchez[1], J. Hernández-Sánchez[1]

[1] *Instituto Politécnico Nacional, Grupo Ingeniería de Superficies, SEPI-ESIME, U.P. Adolfo López Mateos, Zacatenco, Mexico D.F., 07738, Mexico*
[2] *Tecnológico de Monterrey, Campus Estado de México, Carretera al Lago de Guadalupe km 3.5. Atizapán de Zaragoza, 52926, Mexico*
[3] *Instituto Politécnico Nacional, Centro de Nanociencias y Micro y Nano Tecnologías, U.P. Adolfo López Mateos, Zacatenco, Mexico D.F., 07738, Mexico*

Received 6 June 2011, received in revised form 30 December 2011, accepted 2 March 2012

Abstract

The mechanical behavior of AISI 1045 borided steels was evaluated in the present study. The diffusion of boron at the surface of the steel was achieved using the powder-pack method, and the following procedure was employed: a) boron diffusion was conducted at 1223 K for 1 and 3 h, b) boriding was performed at the aforementioned temperature and treatment times, and a subsequent heat treatment (quenching and tempering) was applied. First, the mechanical performance of AISI 1045 borided steels was established by conducting fatigue rotating bending tests in the 150 to 250 MPa range to verify the influence of the Fe_2B layer on the steel surface and to determine the effects of post-heat treatment on borided specimens. Likewise, the Young's modulus, hardness, and yield strength were estimated by performing Berkovich nanoindentation tests on the Fe_2B layer and diffusion zone, and applied loads of 500 and 100 mN were employed, respectively. Another set of indentation marks were produced under loads of 50, 100 300 and 500 mN to evaluate the hardness behavior of the Fe_2B layer as a function of the indentation load. Compared to steel that was not subjected to the diffusion process, the fatigue strength of AISI 1045 borided steel decreased. Moreover, the experimental results revealed that the post-heat treatment did not have an effect on the fatigue performance of the borided samples. In addition, the mechanical properties of the Fe_2B layer and diffusion zone, which were obtained by performing nanoindentation tests, were dissimilar, leading to higher tensile stresses in the layer/diffusion zone interface. Finally, the indentation size effect (ISE) was observed in the Fe_2B layer, and the elastic recovery (ER) model was used to obtain the apparent hardness of the coating.

K e y w o r d s: boriding, borided steel, fatigue strength, hardness, nanoindentation, ISE

1. Introduction

Boriding is an effective thermochemical surface treatment process used to produce hard and wear-resistant coatings on ferrous alloys. In the boriding process, which is performed at temperatures ranging from 973–1273 K over a period of 1–10 h, active boron atoms diffuse into the metal substrate and form metallic boride on the surface of the material. Either one iron boride (Fe_2B) or two iron borides (FeB + Fe_2B) are formed at the substrate surface, depending on the process temperature, chemical composition of the material, boron potential of the medium and boriding time [1].

The case depth is typically matched to the intended industrial application and base material. The optimal boride layer thickness for low-carbon steels and low-alloy steels ranges from 50 μm to 250 μm, whereas the optimal boride layer thickness for high-alloy steels ranges from 25 μm to 76 μm [2, 3].

*Corresponding author: tel.: +52 55 57296000 ext. 54768; fax: +52 55 57296000 ext. 54589; e-mail address: icampos@ipn.mx

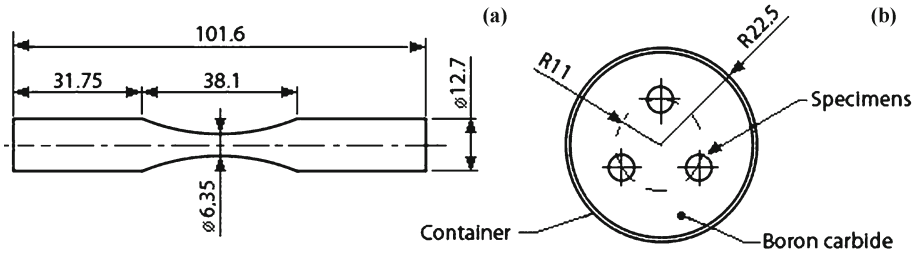

Fig. 1. (a) Standard hourglass-shaped specimens exposed to the boriding process (scale in mm), (b) distribution of the test specimens into the B_4C powder mixture.

In ferrous alloys, the boriding leads to an increase in the specific volume of the boride layer, which increases the fatigue strength of steel. The fatigue strength of borided steels is associated with the brittleness of the boride layer and the distribution of internal stress. Previous works have shown that the behavior of the fatigue strength depends on the heat treatment applied to steel after boriding [4–6].

Indentation tests have been extensively used to measure the mechanical properties of materials. In nanoindentation tests, an indentation is recorded at a high resolution, and the accompanying data are analyzed. The mechanical properties from the load-displacement data are directly analyzed without imaging the indentation. In recent years, the mechanical properties of FeB layer, such as the hardness, Young's modulus and yield strength for AISI 1020 and 1040 borided steels exposed to different conditions during boriding process, have been estimated by performing Dynamic ultra-microhardness testing [7]. According to Culha et al. [7], the load-dependent elastic modulus and hardness of the FeB layer ranges from 125–624 GPa and 17–33 GPa, respectively.

Typically, the measured hardness is high when a low-test load is applied to a ceramic material, and the hardness decreases with an increase in the load [8]. This phenomenon, which is known as the indentation size effect (ISE), depends on the size of the indentation produced from an applied load. Unfortunately, for the hardness values of boride layers, the ISE has not been considered. Therefore, the previously determined hardness values cannot be used as selection criteria for a particular application.

The aims of the present work were as follows:

a) To evaluate the fatigue strength of AISI 1045 steels subjected to powder-pack boriding by performing rotating bending tests. Namely, the fatigue strength of borided steels subjected to a post-heat treatment was compared to that of borided specimens produced without a post-heat treatment.

b) The hardness, Young's modulus and yield strength of the Fe_2B layer and diffusion zone were estimated by performing Berkovich nanoindentation tests on AISI 1045 borided steels produced under different boriding conditions with and without a post-heat treatment.

c) The influence of the ISE on the hardness value of the Fe_2B layer was analyzed using Meyer's law, and the elastic recovery (ER) model was used to obtain the apparent or true hardness of the surface layer.

2. Experimental procedure

2.1. Boriding process

Diffusional boriding was carried out on fifty-six standard hourglass-shaped specimens (ASTM E-739) of commercial AISI 1045 steel (Fig. 1). The samples were embedded in a closed, cylindrical case (AISI 304 L) containing a B_4C *Durborid* fresh powder mixture with a powder size of 50 μm. Boriding was accomplished by placing the container in a furnace in the absence of inert gases, and the boriding time began when the temperature of the furnace reached the boriding temperature. The Fe_2B layers on the surface of the steel were grown at 1223 K for 1 and 3 h. When the treatment was complete, the container was removed from the furnace and was slowly cooled to room temperature. After the boriding process, twenty-eight fatigue borided samples were oil-quenched at 1118 K and were tempered at 478 K for 20 min.

In addition, the same boriding process and heat treatment conditions were applied to cylindrical samples (diameter of 3.125 mm) of AISI 1045 steels to evaluate the evolution of the boride layer as a function of the exposure time. The borided samples were cross-sectioned for metallographic preparation, and the depth of the Fe_2B layer was observed under a clear field using an Olympus GX51 metallurgical microscope. Twenty-five measurements were taken on different sections of borided AISI 1045 samples to estimate the thickness of the Fe_2B layer. The thickness of the Fe_2B layer ranged from 40 ± 11 μm at a boriding temperature of 1223 K and an exposure time of 1 h, while thicknesses of 80 ± 13 μm were observed at a boriding temperature of 1223 K and an exposure time of 3 h, as shown in Fig. 2. These samples were subjected to Berkovich nanoindentation tests.

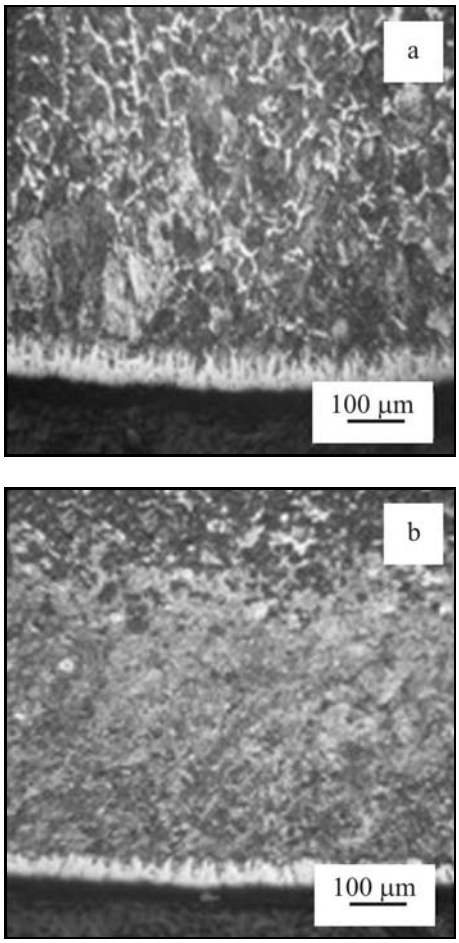

Fig. 2. Evolution of the Fe_2B layers as a function of the exposure time: (a) 3 h, (b) 1 h.

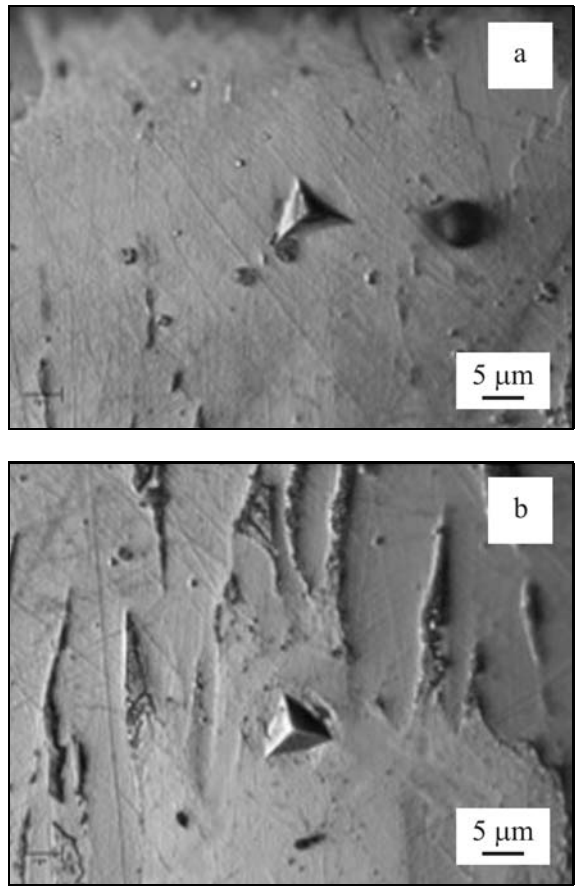

Fig. 3. Berkovich indentation marks produced at: (a) the Fe_2B layer at an applied load of 500 mN and (b) the diffusion zone at an applied load of 100 mN.

2.2. Fatigue testing

The effects of the boriding process and heat treatment on the fatigue strength of AISI 1045 borided steels were studied on samples (diameter of 6.35 mm) fatigued in rotating bending ($R = -1$) tests, which were performed at room temperature on a RBF 200 machine at a speed of 4000 rpm. The surface roughness of the borided samples was estimated to be 0.20 µ. In accordance with ASTM E-739, the magnitude of stresses applied on the samples ranged from 150 MPa to 250 MPa, and the tests were finished when the specimens were completely fractured. In addition, the fatigue fractures of the samples were analyzed using a JEOL JSM 6360 LV scanning electron microscope.

2.3. Berkovich nanoindentation testing

Berkovich nanoindentation tests were carried out using a nanohardness tester (TTX-NHT, CSM Instruments). The nanoindentations were applied to AISI 1045 borided steel specimens produced under different boriding conditions with and without a post-heat treatment. The nanoindentations were performed on the Fe_2B layer (20 µm from the surface of the material) and the diffusion zone (underneath the boride layer), and a load of 500 and 100 mN was applied, respectively (Fig. 3). The distance between adjacent indentation marks was at least 4 times greater than the diagonal-length mark to ensure that the indentation marks did not interact with each other. For a particular load, twenty load-displacement curves were recorded automatically and were analyzed according to the Oliver-Pharr procedure to assess the evolution of hardness and Young's modulus as a function of the load and contact depth. The Poisson's ratio of the Fe_2B layer was set to 0.3 [9]. Representative results of the load-displacement curves are presented in Fig. 4.

In addition, to analyze the ISE on the hardness values of the Fe_2B layer, Berkovich nanoindentations were performed 20 µm from the surface of the borided steel, and loads of 50, 100, 300 and 500 mN were applied to specimens produced under various boriding and post-heat treatment conditions, as depicted in Fig. 5.

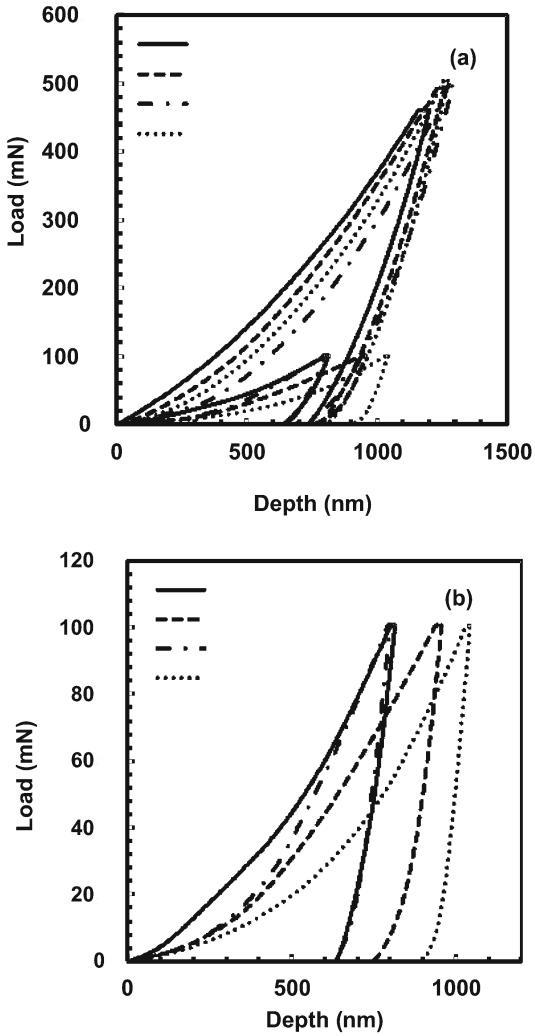

Fig. 4. Load-displacement plots for (a) the Fe_2B layer and (b) the diffusion zone. — borided for 1 h and exposed to heat treatment, – – borided for 1 h, – · – borided for 3 h and exposed to heat treatment, ··· borided for 3 h.

3. Results and discussion

The diffusion of boron through the Fe_2B layer was strongly anisotropic, as stated by Brakman et al. [10]. Consequently, jagged interfaces were observed between the steel and the boride layer. Ninham and Hutchings [11] suggested that the columnar nature of the coating interface is caused by dendritic side arm growth, which is similar to that observed during the solidification process of many metallic systems. In low-carbon steels, the boride may break through the impurity bands, which allows rapid local boride growth and results in a saw-toothed interface.

Comparing the results of fatigue strength in the finite region (Fig. 6) of samples not exposed to the boriding process, it seems that the diffusion process reduced the fatigue life of the AISI 1045 borided steels.

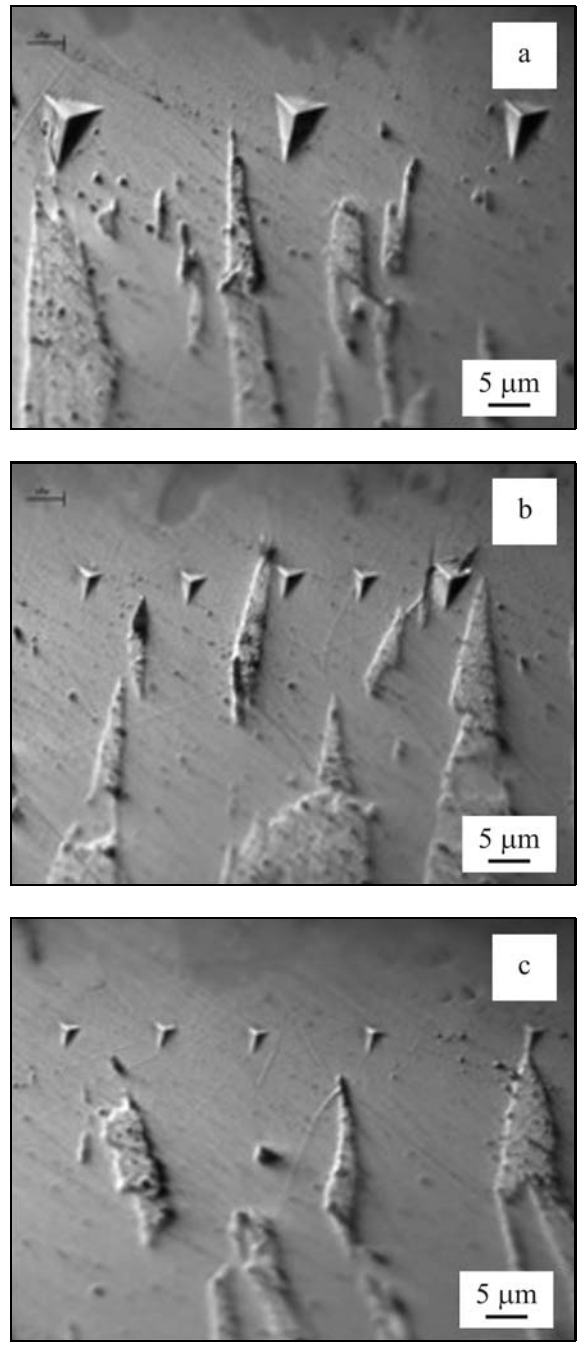

Fig. 5. Berkovich indentation marks on the Fe_2B layer at applied loads of: (a) 300 mN, (b) 100 mN and (c) 50 mN.

This phenomenon can be attributed to both the brittleness of the boride layer and the internal stress distribution [4]. Moreover, that post-heat treatment did not affect the fatigue strength of borided steels. The observed reduction in the fatigue strength of borided steels was associated with the jagged structure of the boride layer, which contained brittle precipitates at the grain boundaries [12]. Tensile stresses, which reach their maximum in rotating bending tests, lead to the

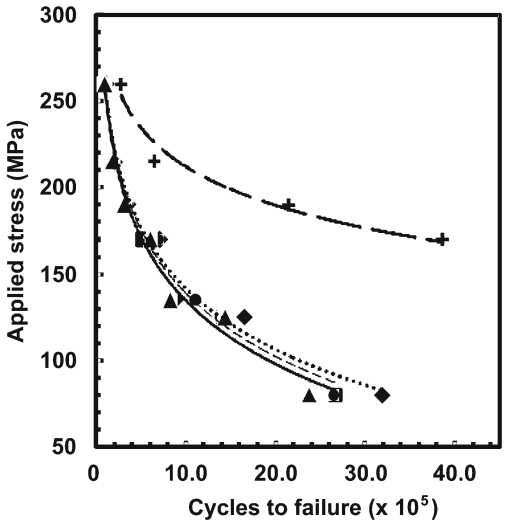

Fig. 6. Results of rotating bending fatigue tests carried out on borided and non-borided specimens: + AISI 1045 steel, ■ borided for 1 h, ◆ borided for 1 h and exposed to heat treatment, ● borided for 3 h, ▲ borided for 3 h and exposed to heat treatment.

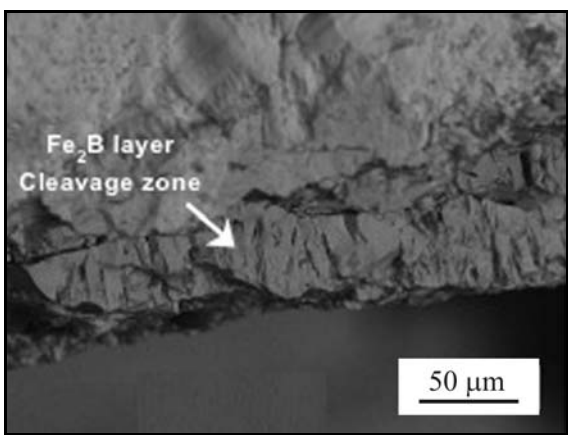

Fig. 7. Cross-sectional view of the fracture surface of AISI 1045 borided steel subjected to the rotating bending fatigue test.

nucleation of intercrystalline fatigue cracks. The formation of tensile regions is a function of the grade of curvature of the boride layer/substrate interface and their complicated geometry [13]. The fatigue fracture of borided steel, as depicted in Fig. 7, showed that crack advancement due to external loading was proportional to the maximum applied stress. Thus, the mechanism of fracture in the Fe_2B layer was cleavage.

The mechanical properties such as the Young's modulus (E), yield strength (σ_y) and hardness (H) of the Fe_2B layer and diffusion zone of AISI borided steels and borided steels exposed to the quenching and tempering treatments were determined by performing Berkovich nanoindentation tests, and the results are summarized in Table 1. The Young's modulus of the Fe_2B layer and diffusion zone was recorded according to the Oliver and Pharr method from the unloaded zone of the load-displacement curve. Alternatively, the yield strength was obtained using the equation proposed by Tabor [14] ($\sigma_y = H/3$). Furthermore, the ratio E/σ_y of both zones can be considered as the "ductility" of the coating/substrate system. Namely, dissimilar values lead to a higher state of tensile stresses in the layer/diffusion zone interface. As shown in Table 1, the post-heat treatment increased the mechanical properties of the diffusion zone due to the presence of a martensitic phase, which reduced the hardness gradient of the Fe_2B layer to the substrate. In addition, several authors [10, 15] have shown that carbon present in steel does not dissolve at the boride layers and diffuses away from the surface, forming a layer of borocementite beneath the boride layer.

The evolution of the hardness as a function of the applied load of the Fe_2B layer at a constant distance (20 μm) from the surface of borided steel is plotted in Fig. 8. The results shown in Fig. 8 reveal that the hardness decreased with an increase in the applied load. ISE has been traditionally described using Meyer's law [16]:

$$P_{\max} = Ah_c^n, \tag{1}$$

where h_c is the contact depth of the indenter with the

Table 1. Mechanical properties obtained by Berkovich nanoindentation tests performed on the Fe_2B layer and the diffusion zone

Sample	Fe_2B layer				Diffusion zone			
	H (GPa)	E (GPa)	σ_y (GPa)	E/σ_y	H (GPa)	E (GPa)	σ_y (GPa)	E/σ_y
1	18.7 ± 1.0	296 ± 6.2	6.2	47.7	9.6 ± 1.7	255 ± 18	3.2	79.6
2	19.6 ± 0.2	294 ± 6.3	6.5	45.2	4.5 ± 0.8	242 ± 27	1.5	161.3
3	18.8 ± 1.2	285 ± 16.7	6.2	45.9	6.8 ± 0.8	235 ± 28	2.2	106.8
4	18.3 ± 0.4	300 ± 12.2	6.1	49.1	4.4 ± 1.0	247 ± 33	1.4	176.4

1 – boriding for 1 h and exposed to heat treatment, 2 – boriding for 1 h, 3 – boriding for 3 h and exposed to heat treatment, 4 – boriding for 3 h

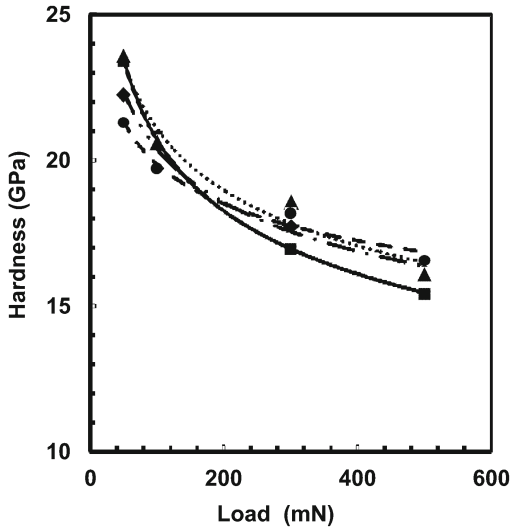

Fig. 8. Variation in the hardness values obtained of the Fe_2B layer as a function of indentation loads: ◆ borided for 1 h and exposed to heat treatment, ■ borided for 1 h, ▲ borided for 3 h and exposed to heat treatment, ● borided for 3 h.

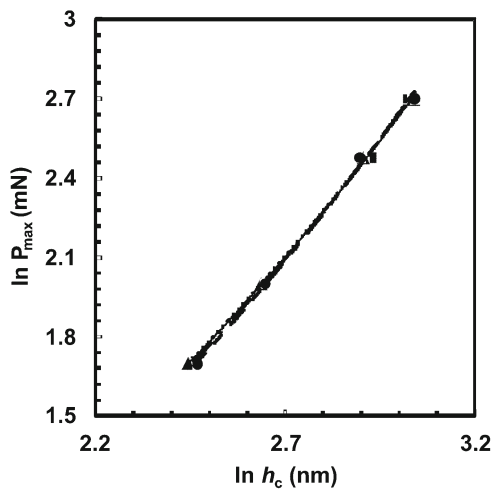

Fig. 9. The dependence of the applied load as a function of the contact depth: ◆ borided for 1 h and exposed to heat treatment, ■ borided for 1 h, ▲ borided for 3 h and exposed to heat treatment, ● borided for 3 h.

sample at P_{max}, and A and n are constants derived from the curve fit of the plot on a bilogarithmic scale. The value of n (or the Meyer index) that characterizes the curve, is often referred to as the ISE. This effect is especially apparent in hard, brittle ceramics at low indentation loads, where n is significantly less than 2. When $n > 2$, the hardness increases with an increase in the applied load. When $n = 2$, the hardness is independent of the applied load and P_{max} is given by Kick's law [17]:

Table 2. Best fit-values of the parameters in Eq. (1) for AISI 1045 borided steels subjected to different boriding conditions

Sample	Parameters in Eq. (1)		
	A (mN nm^{-n})	n	R^2
1	0.0026	1.742 ± 0.0215	0.9997
2	0.0034	1.700 ± 0.0651	0.9971
3	0.0035	1.698 ± 0.0293	0.9994
4	0.0020	1.776 ± 0.0400	0.9990

1 – boriding for 1 h and exposed to heat treatment, 2 – boriding for 1 h, 3 – boriding for 3 h and exposed to heat treatment, 4 – boriding for 3 h

$$P_{max} = Ah_c^2, \tag{2}$$

where A is the standard hardness constant.

Furthermore, the behavior of the applied load as a function of the contact depth was plotted according to Meyer's law (Eq. (1)), as shown in Fig. 9. The linear regression results, which are summarized in Table 2, indicated that the n values were less than two, which confirmed the presence of ISE in the Fe_2B layer. ISE was attributed to the small size of the indentation (typically 1 to 10 μm) and various intrinsic structural factors of the tested specimens [18].

The apparent or true hardness (H_o) of the Fe_2B layer was estimated according to the ER model. This model is based on the elastic recovery of the material when the indenter is removed from the surface. The elastic recovery of the indenter indicates that the contact depth should be reduced by a certain degree [19–21]; therefore, the measured contact depth must be corrected using a revised term to obtain the true hardness, as shown in the following equation:

$$H_o = k\frac{P_{max}}{(h_c + h_o)^2}, \tag{3}$$

where h_o is the correction factor for the contact depth h_c due to elastic recovery and k is a constant that is dependent on the indenter geometry.

Thus, Eq. (3) can be modified as follows:

$$P_{max}^{1/2} = \chi^{1/2}h_c + \chi^{1/2}h_o, \tag{4}$$

where $\chi = H_o/k$. From a plot of $P_{max}^{1/2}$ versus h_c, h_o and χ can be estimated.

The results obtained from the ER model, which was based on a plot of $P^{1/2}$ versus h_c (Fig. 10), indicated that the correlation factor was high. In addition, the best-fit values of the correction factor h_o on the indentation size h_c and the parameter χ are shown in Table 3. The apparent hardness of the Fe_2B layer

Table 3. Parameters of the ER model obtained by nanoindentation, which was performed 20 μm from the surface of AISI 1045 borided steels

Sample	χ (mN nm^{-2}) $\times 10^{-2}$	h_o (nm)	R^2	H_o (GPa)
1	1.936 ± 0.018	79.75	0.9998	15.31 ± 0.0014
2	1.922 ± 0.079	83.42	0.9965	15.09 ± 0.0260
3	1.892 ± 0.031	95.53	0.9994	14.62 ± 0.0041
4	1.930 ± 0.072	78.66	0.9971	15.22 ± 0.0213

1 – boriding for 1 h and exposed to heat treatment, 2 – boriding for 1 h, 3 – boriding for 3 h and exposed to heat treatment, 4 – boriding for 3 h

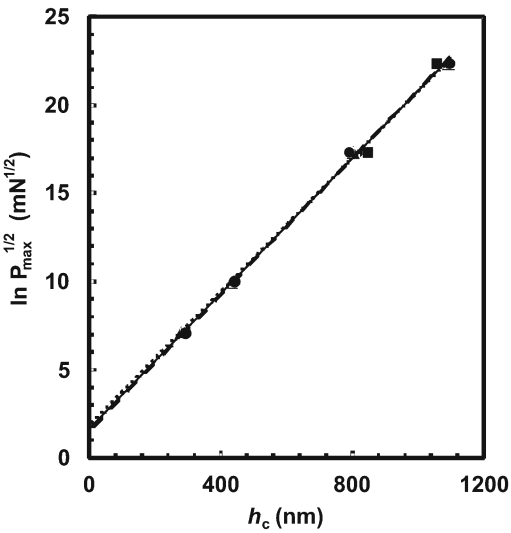

Fig. 10. Berkovich nanoindentation data obtained from the Fe_2B layer, according to the ER model: ◆ borided for 1 h and exposed to heat treatment, ■ borided for 1 h, ▲ borided for 3 h and exposed to heat treatment, ● borided for 3 h.

estimated by the ER model was not affected by the post-heat treatment and the boriding exposure time and ranged from 14.2 GPa to 15.3 GPa.

4. Conclusions

The mechanical behavior of AISI 1045 steels exposed to the boriding process was estimated in the present study. The fatigue strength of borided steels and borided specimens exposed to post-heat treatment was reduced compared to non-borided steels due to the brittleness of the boride layer and the presence of tensile stresses at the saw-toothed Fe_2B/diffusion zone interface. Likewise, the diffusion zone of borided steels was only affected by post-heat treatment, which increased the mechanical properties of the material, including the Young's modulus, yield strength and hardness, which were determined by performing Berkovich nanoindentation tests. Hardness measurements on the Fe_2B layer at a distance of 20 μ from the surface of the borided steel were dependent on the applied load, and the ISE could be described by Meyer's law and the ER model. In the ER model, the estimated apparent hardness of the Fe_2B layer ranged from 14.2 GPa to 15.3 GPa as a function of the experimental conditions of the boriding process.

Acknowledgements

This work was supported by the research grants 150556 of the CONACYT and 20120594 of the Instituto Politécnico Nacional of México. The authors wish to thank the Nanosciences Center and Micro-Nano Technologies of the Instituto Politécnico Nacional for their cooperation.

References

[1] Campos-Silva, I., Ortiz-Domínguez, M., Keddam, M., López-Perrusquia, N., Carmona-Vargas, A., Elias-Espinosa, M.: Appl. Surf. Sci., *255*, 2009, p. 9290. doi:10.1016/j.apsusc.2009.07.029
[2] Graf von Matuschka, A.: Boronizing. Munich, Carl Hanser Verlag 1980.
[3] Campos-Silva, I., Ortiz-Domínguez, M., Cimenoglu, H., Escobar-Galindo, R., Keddam, M., Elias-Espinosa, M., López-Perrusquia, N.: Surf. Eng., *27*, 2011, p. 189.
[4] Gurevich, B. G., Pirogova, V. A.: Fisiko-Khimicheskaya Mekhanika Materialov, *6*, 1967, p. 693.
[5] Zamikhovskii, V. S., Pokhmurskii, V. I., Karpenko, G. V.: Fisiko-Khimicheskaya Mekhanika Materialov, *3*, 1967, p. 182.
[6] Celik, O. N., Gasan, H., Ulutan, M., Saygin, M.: J. Achiev. Mater. Manuf. Eng., *32*, 2009, p. 13.
[7] Culha, O., Toparli, M., Sahin, S., Aksoy, T.: J. Mater. Process. Technol., *206*, 2008, p. 231. doi:10.1016/j.jmatprotec.2007.12.020
[8] Quinn, J. B., Quinn, G. D.: J. Mater. Sci., *32*, 1997, p. 4331. doi:10.1023/A:1018671823059
[9] Frantzevich, N., Voronov, F. F., Bakuta, S. A.: Elastic Constants and Elastic Modulus for Metals and Non-Metals: Handbook. Kiev, Naukova Dumka Press 1982.
[10] Brakman, C. M., Gommers, A. W. J., Mittemeijer, E. J.: Mater. Res., *4*, 1989, p. 1354. doi:10.1557/JMR.1989.1354
[11] Ninham, A. J., Hutchings, I. M.: J. Vac. Sci. Technol. A, *4*, 1986, p. 2827. doi:10.1116/1.573686

[12] Mikhailov, P. A., Ponomarenko, E. P., Petergerya, D. M., Domio, A. A., Rybkin, V. F., Khokhlov, V. P., Kasyanenko, V. G.: Fisiko-Khimicheskaya Mekhanika Materialov, *4*, 1968, p. 133.
[13] Balokhonov, R. R., Romanova, V. A.: Int. J. Plasticity, *25*, 2009, p. 2025. doi:10.1016/j.ijplas.2009.01.001
[14] Tabor, D.: Hardness of Metals. Oxford, Clarendon Press 1951.
[15] Campos-Silva, I., Ortiz-Dominguez, M., Villavelazquez, C., Escobar, R., Lopez, N.: Defect and Diffus. Forum, *272*, 2007, p. 79.
[16] Gong, J., Wu, J., Guan, Z.: J. Mater. Sci. Lett., *17*, 1998, p. 473. doi:10.1023/A:1006576326731
[17] Zewen, W., Wanqi, J.: Mater. Sci. Eng. A, *452–453*, 2007, p. 508. doi:10.1016/j.msea.2006.10.079
[18] Iost, A., Bigot, R.: J. Mater. Sci., *31*, 1996, p. 3573.
[19] Atkinson, M.: J. Mater. Sci., *30*, 1995, p. 1728. doi:10.1007/BF00351602
[20] Tarkanian, M. L., Neumann, J. P., Raymond, L.: The Science of Hardness Testing and its Research Applications. Ohio, ASM International 1973.
[21] Peng, Z., Gong, J., Miao, H.: J. Eur. Ceram. Soc., *24*, 2004, p. 2193. doi:10.1016/S0955-2219(03)00641-1